Acta Crystallographica Section B
Structural Science
ISSN 0108-7681

Pseudoepitaxial transrotational structures in 14 nm-thick NiSi layers on [001] silicon

Alessandra Alberti,[a]* Corrado Bongiorno,[a] Brunella Cafra,[a] Giovanni Mannino,[a] Emanuele Rimini,[a] Till Metzger,[b] Cristian Mocuta,[b] Thorsten Kammler[c] and Thomas Feudel[c]

[a]CNR-IMM, Sezione di Catania, Stradale Primosole 50, 95121 Catania, Italy, [b]European Synchrotron Radiation Facility, BP 220, 38043 Grenoble CEDEX, France, and [c]AMD Saxony LLC and Co. KG, Wilschdorfer Landstrasse 101, Dresden, Germany

Correspondence e-mail:
alessandra.alberti@imm.cnr.it

Received 16 March 2005
Accepted 14 July 2005

In a system consisting of two different lattices, structural stability is ensured when an epitaxial relationship occurs between them and allows the system to retain the stress whilst avoiding the formation of a polycrystalline film. The phenomenon occurs if the film thickness does not exceed a critical value. Here we show that in spite of its orthorhombic structure, a 14 nm-thick NiSi layer can three-dimensionally adapt to the cubic Si lattice by forming *transrotational* domains. Each domain arises by the continuous bending of the NiSi lattice, maintaining a close relationship with the substrate structure. The presence of *transrotational* domains does not cause a roughening of the layer, but instead it improves the structural and electrical stability of the silicide in comparison with a 24 nm-thick layer formed using the same annealing process. These results have relevant implications for the thickness scaling of NiSi layers which are currently used as metallizations of electronic devices.

1. Introduction

Low-resistivity nickel silicide (NiSi) will replace cobalt silicide in the next-generation metal-oxide-semiconductor devices (MOSFET). The main advantage of NiSi is the reduction of Si consumption without an increase in the sheet resistance in order to ensure shallow junction integrity and low contact resistance. In this respect, it is mandatory to avoid the transition of NiSi to the high-resistivity $NiSi_2$ phase as the annealing temperature exceeds 973–1073 K (Teodorescu *et al.*, 2001; Lavoie *et al.*, 2003; Lauwers *et al.*, 2001) and to control the interfacial properties (Choi *et al.*, 2002; Wong *et al.*, 2002; Ok *et al.*, 2003; Lee *et al.*, 2003; Lauwers *et al.*, 2004). A general method to optimize the structure of the silicide layer consists of reducing the interfacial free energy between the layer and the substrate and/or increasing the volume energy gain of the nucleation barrier (Chen & Tu, 1991). Recently, it has been shown that, in spite of the lattice dissimilarity of the orthorhombic NiSi with cubic Si, an ordered relationship between the silicide layer and the substrate is established; this peculiar growth was called axiotaxy (Detavernier *et al.*, 2003; Detavernier & Lavoie, 2004). Axiotaxy represents an intermediate case between heteroepitaxy and a random growth; it is a fibre-like texture but with an off-normal fibre axis resulting in a one-dimensional periodic interface.

In this work we show that the NiSi lattice can three-dimensionally adapt to the Si lattice by forming *transrotational* domains. This phenomenon has been observed for reaction temperatures between 533 and 1173 K in pure nitrogen and in a vacuum, by using rapid thermal annealing (spike or 30 s) and furnace annealing, on Cz–Si and Silicon-on-Insulator (SOI) substrates. The resulting structural properties of the silicide

© 2005 International Union of Crystallography
Printed in Great Britain – all rights reserved

layer are promising to improve the structural and electrical stability of NiSi.

2. Experimental

On [001] Cz–Si cleaned substrates, 7 nm-thick nickel layers were deposited by sputtering and then subsequently annealed in a Rapid Thermal Annealer (RTA) for 30 s, or by spike annealing in pure nitrogen ambient between 723 and 1173 K, or by furnace annealing in the range 533 and 623 K. The reacted samples were analysed by X-ray diffraction (XRD), Transmission Electron Microscopy (TEM) and Selected Area Diffraction (SAD). Pole figures were measured at the ID01 beamline of the European Synchrotron Radiation Facilities (ESRF) in Grenoble using a photon energy of E = 8 keV (Cu $K\alpha$) to study the three-dimensional configuration of the NiSi lattice with respect to the substrate.

3. Results and discussion

Here we report on the structure of a 14 nm NiSi layer formed after spike annealing at 823 K, as representative of all the samples described above. Fig. 1(*a*) is a large-area plan-view TEM image of the silicide layer taken at a 5° tilt with respect to the [001] Si direction to reduce the substrate contributions. The pattern does not match that of a conventional polycrystalline film since the boundaries between adjacent domains are not clearly defined. On the contrary, an intricate network of extinction contours covers the entire area of the sample. The extinction contours create some peculiar, highly ordered and symmetric structures defined by the intersection of more than two fringes, as indicated by the dashed ellipses in Fig. 1(*a*). A thicker silicide layer (24 nm), formed under the same annealing conditions, has the structure of a conventional polycrystal instead, as shown in Figs. 1(*c*) and (*d*).

A network of extinction contours was first observed by Kolosov & Thölen (2000) in crystalline Se or Fe-based spherulites in an amorphous matrix, and subsequently in the crystallization of amorphous chalcogenide films (Kooi & De Hosson, 2002, 2004; Kooi *et al.*, 2004). In these studies it was determined that the domains, defined by the intersection of extinction contours, were generated by a continuous rotation of the crystal that bends without producing a roughening of the interfaces (*transrotational structures*; Kolosov & Thölen, 2000). Likewise, we have found that within each domain the lattice of NiSi bends around a fixed zone axis following an almost hemispherical path. The centre of the domain, at the intersection of the extinction contours, is the only region in which the lattice is in the axis condition. It has been observed that by tilting the sample, the centre of the intersection between the contours moves in the same direction as the tilt, and from this property it is possible to determine the sign of the curvature of these domains. The domains have been found to be concave. In contrast to the chalcogenides (Kooi & De Hosson, 2004), our films have a tight relationship with the substrate which is not amorphous but crystalline.

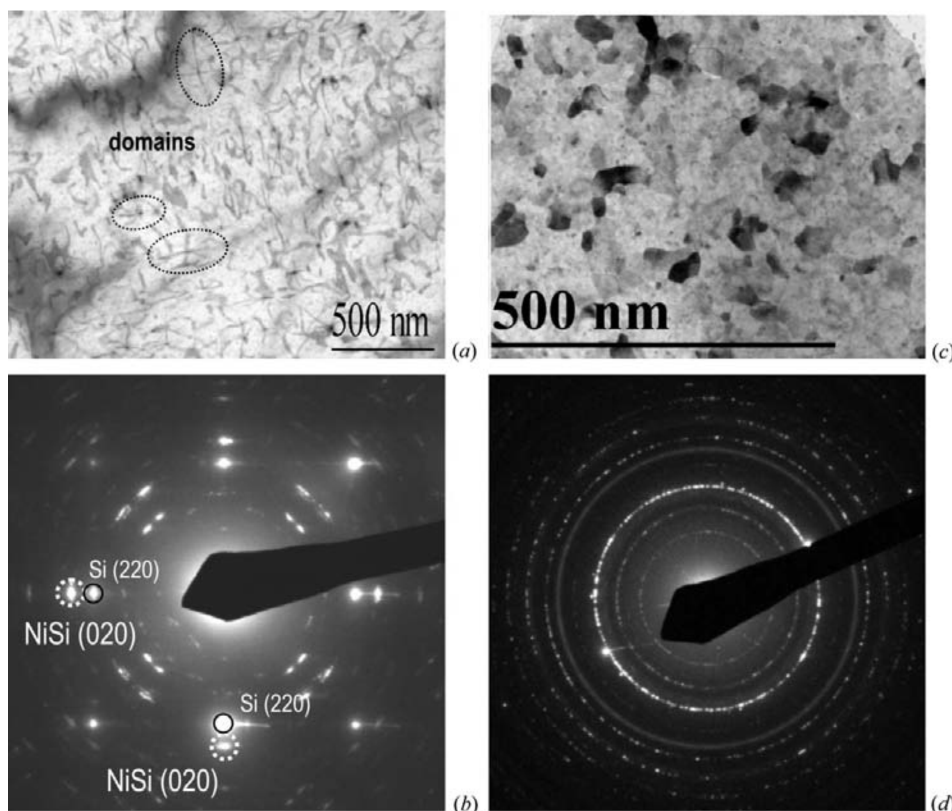

Figure 1
Structural analyses. (*a*) Plan-view TEM image of a 14 nm-thick silicide layer reacted by spike annealing at 823 K. An intricate network of extinction contours (black lines) covers the entire area of the sample. Domains are defined by the intersection of more than two of those contours. (*b*) Large-area diffraction analysis showing the location of (020) planes of NiSi with respect to the Si lattice structure. These planes, which are perpendicular to the sample surface, have only two allowed configurations at 90° to each other (see the dashed circles). (*c*) Plan-view image and (*d*) large-area diffraction analysis of a 24 nm-thick NiSi layer obtained by spike annealing at 823 K.

The electron diffraction pattern shown in Fig. 1(*b*) is characterized by two intense spots, perpendicular to each other, aligned to the [220] directions of the substrate. They are due to the unique (020) planes of the NiSi orthorhombic lattice and they therefore belong to different zone axes rotated by 90°.

To fully characterize the relationship between the film and the substrate, SAD analyses have been performed on different domains of the sample. It is noteworthy that all the collected diffraction patterns can be associated to three different zone axes, *i.e.* the [101], [102] and [201] directions of the NiSi lattice. Each of these zone axes has been associated with a particular domain, characterized by a different number and the mutual position of the extinction contours. The last two zone axes have similar diffraction patterns and therefore the associated domains are not easily distinguishable in the plan-view image. The main domains, identified as type I (Fig. 2*a*) and type II (Fig. 2*b*), are formed by the intersection of four or three fringes, respectively (type III not shown). It is worth noting that the extinction contours are almost perpendicular to the diffraction spots labelled in the corresponding SAD (right side of Fig. 2) and this confirms the *transrotational* structure of the domains. All the intense spots in Fig. 1(*b*) are reproduced by these patterns and by those rotated by 90°. This implies that, within the large area analysed, the film shows primarily three types of domain orientation. The peculiarity of this kind of growth is the close relationship between the lattices of NiSi and Si in which, within each bending contour of the domain, the (020) planes of the silicide are anchored at the interface with silicon to its (220) planes. A schematic view of the planes bending along one direction is sketched in Fig. 2(*c*).

A ±18° continuous rotation of the orthorhombic NiSi lattice around the direction normal to the (020) planes moves the lattice configuration from the [102] to the [201] zone axis, passing through [101] without meeting other relevant axes in-between. This result, combined with the presence of the bending contours within the domains, suggests that along the (020) related fringes the lattice of NiSi is able to bend in a continuous way, preserving the (020) planes aligned to the (220) planes of the substrate. This kind of preferential alignment is lost immediately outside the (020) fringes in all the other directions, as sketched in Fig. 2(*c*). Therefore, the continuous rotational configurations of the NiSi lattice around the (020) planes, from one zone axis to another, are all present within a single *transrotational* domain rather than being associated with a collection of differently oriented domains.

In order to investigate the spatial distribution of these preferentially oriented fringes, dark-field TEM analyses were performed over the sample area shown in Fig. 1(*a*) by selecting each of the two [020] spots of the diffraction pattern labelled in Fig. 1(*b*). Two clearly distinguishable and spatially separated sets of bright fringes were detected over the entire sample area. The first set of fringes, shown in Fig. 3(*a*), covers the upper part of the sample area; the second set of fringes, rotated by 90°, occupies the lower part of the analysed area (Fig. 3*b*). These planes follow the symmetry of (220) planes of silicon.

The statistical angular distribution of the (020) NiSi planes was obtained by X-ray diffraction analysis, altering the azimuthal angle φ from 0 to 360° and the polar angle χ from 0

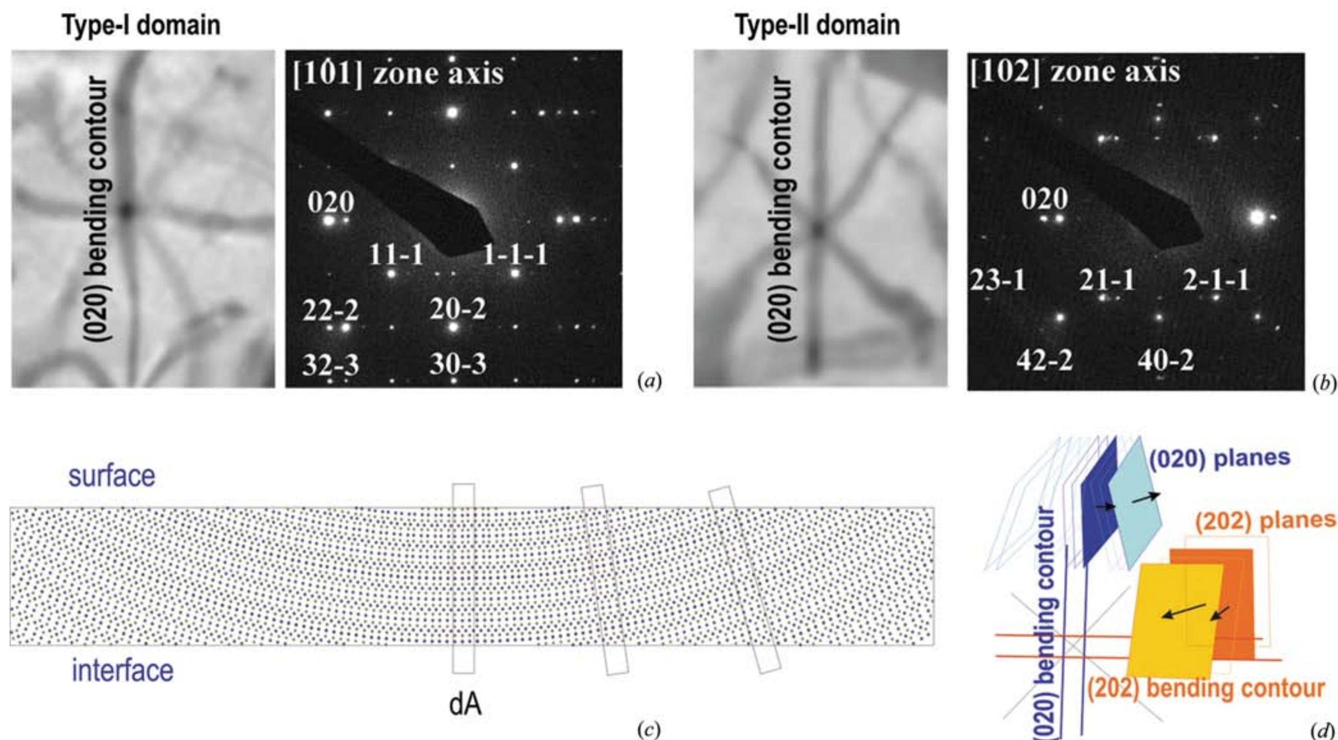

Figure 2
Domain structure. Details of (*a*) type I and (*b*) type II domains defined on the basis of the corresponding SAD patterns. The extinction contours are almost perpendicular to the diffraction spots labelled in the corresponding SAD and in these regions the NiSi planes are in Bragg conditions. This condition is lost outside the contours due to the continuous bending of the NiSi planes, as sketched in (*c*). The bending occurs in all directions, as represented in the case of the (020) and (202) NiSi planes shown in (*d*), changing the properties of the interface without producing structural roughnening of the layer.

to 86°. The resulting stereo projection is shown on a logarithmic colour scale in Fig. 4(*a*). The intensity distribution consists of well defined regions placed in symmetrical positions. For the selected wavelength and Bragg angle, the pole figure contains contributions from the (020) and (013) planes of the NiSi film and the (311) planes of the substrate, all having similar *d*-spacing (d = 1.629, 1.632 and 1.637 Å, respectively). The signals of the substrate are identified by dark squares in Fig. 4(*a*) and are located at χ = 26 and 72°, with a distribution along φ, which follows the symmetry of the silicon lattice. The remaining intense patterns are due to the NiSi layer. Their distribution and shape cannot be accounted for by either a random growth, or epitaxy or axiotaxy. Random growth should, in fact, result in a uniform angular intensity distribution; epitaxy should produce a small rounded pattern corresponding to the substrate planes; axiotaxy should give circular features in the spherical representation around χ = 45° and φ = 45, 135, 225 and 315° (Detavernier *et al.*, 2003; Detavernier & Lavoie, 2004). The presence of narrow elongated patterns at φ = 0, 90, 180 and 270° that follow the symmetry of the (220) Si planes is noteworthy. They extend by only 4° along φ and from 86 to 70° along χ. These contributions have been related to the (020) planes of NiSi. Other extended features are found in the proximity of χ = 45° and φ = 45, 135, 225 and 315°. Each of them is lozenge-shaped, as shown with quadrant IV of the pole figure, and is related to the (013) planes of NiSi. The sketch in Fig. 4(*b*), representing a row of domains, can be used to explain the distribution and shape of all the diffraction patterns attributed to the NiSi lattice. Starting with the core of the type I domain, labelled 'A' and corresponding to the [101] zone axis, the core 'C' of a type II domain is obtained by the continuous rotation of the NiSi lattice around the direction normal to the (020) planes. These planes indeed remain in the same position. The rotation causes, instead, all the (013) planes to move according to their mutual position in the NiSi lattice and therefore to contribute to the diffraction pattern in different positions. The related diffracted spots are represented with quadrants I and II of the pole figure, and they move from the black to the blue positions passing through the red positions. These movements of the lattice do not produce any shift of the (020) spots, which remain at φ = 0° and χ = 90° (black, red and blue circles are superimposed). Following the *transrotational* structure of each domain (Fig. 2), other representative lattice configurations are obtained and represented with the corresponding colours. When the lattice lies in the 'E', 'F', 'D', 'G' configurations, the (020) spot moves along χ (yellow circle) or slightly apart from this axis (the other colours). Some representative configurations within the type III domains have also been considered ('C′, D′, F′') and represented as dashed circles with quadrant II. According to the results shown in Fig. 3, the contributions of the same row of domains rotated by 90° have additionally been represented with quadrant III. In this way, half of the lozenge-shaped pattern is covered by the coloured circles, the other symmetric side being completed by representing the right part of the domains (not superimposed). The corresponding (020) spots tend to cover the elongated patterns at the edge of the pole figure describing, indeed, the bending of the (020) planes outside the related extinction contour. The higher intensity of the central part of these patterns is due to the size and shape of the domains. The analysis of this pole figure proves that the locations of the (013) planes of NiSi are in a tight relationship with the *transrotational* structures of the domains and also that these planes assume a continuous but limited number of configurations.

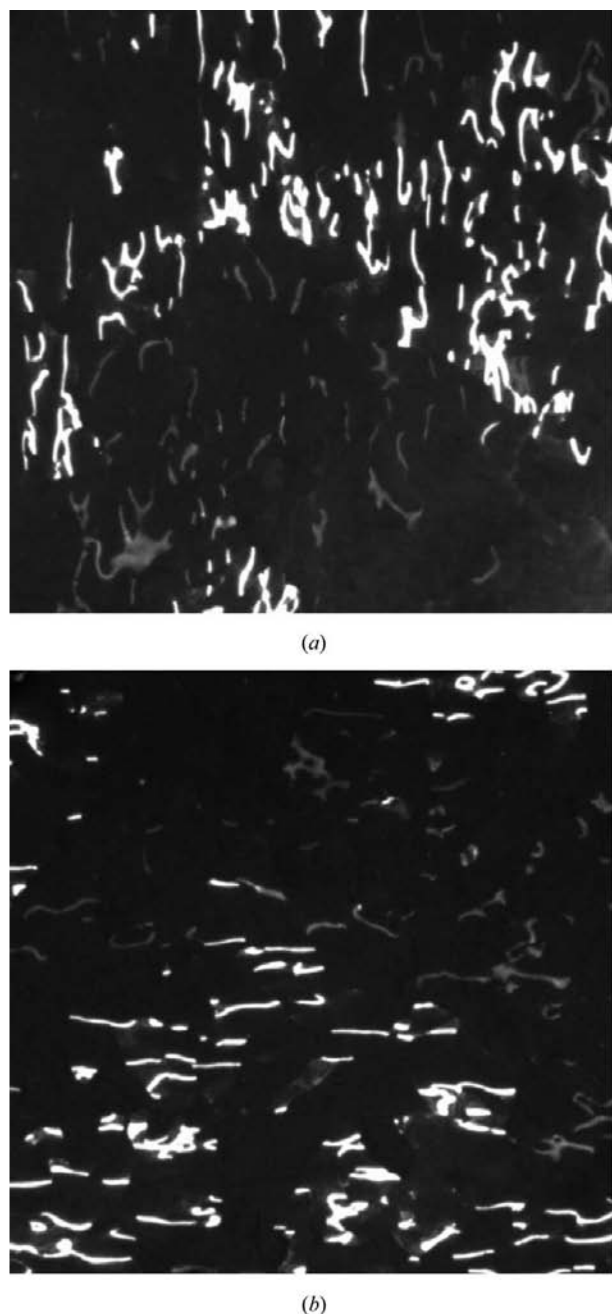

Figure 3
(020) NiSi bending contours. Dark-field TEM analyses obtained by selecting each of the outlined [020] spots in Fig. 1(*b*). The upper part of the sample has domains with similarly oriented (020) bending contours (*a*). The domains in the lower part have the (020) bending contours rotated by 90° (*b*). Therefore, two regions are defined on the basis of the orientation of these contours and they cover the entire area of the sample.

To further support and extend these results, the pole figure of the (202)/(211) planes of NiSi has been analysed with the appropriate choice of Bragg angle, and the results are shown in Fig. 5. These two sets of planes, and also the (220) planes of silicon, are undistinguishable due to their similar *d*-spacing. This pole figure is characterized by four extended patterns located at $\varphi = 0, 180, 270$ and 360°, which have been attributed to the (202) planes of NiSi. Another four symmetrical lozenge-shaped contributions, centred at $\chi = 45^\circ$ and $\varphi = 45, 135, 225$ and 315°, were found, each having two splitting arms which extend towards the edge of the figure. The core of these patterns is due to the (220) Si planes, as indicated by the black squares in Fig. 5. The further extension of these large patterns unambiguously establishes the presence of continuous contributions from the (211) planes of the silicide layer. Following the domain structure sketched on the left side of Fig. 5, some representative contributions given by (211) and (202) NiSi planes are represented in the pole figure by coloured circles. They also represent contributions from a similar row of domains rotated by 90° (see Fig. 3). The diffracted spots accumulate within the lozenge-shaped features and also reproduce their splitting arms. In correspondence, the (202) planes move along and in proximity to the χ axis as a consequence of the (020) planes bending outside the related bending contours.

Our findings significantly support the *transrotational* nature of the domains and, moreover, we conclude that the entire NiSi layer has grown following these structures. In addition, the analysis of the poles introduces a new description of the growth of NiSi which substantially differs from axiotaxy (Detavernier *et al.*, 2003). Let us consider the three-dimensional pseudomatch sketched on the right side of Fig. 5, in which a double relationship between the lattices of NiSi and Si is established. It consists of a couple of (211) planes of NiSi which lie, except for a tilt in χ, on the (220) planes of Si which cross the diagonal of the cube faces. The positions of these NiSi planes in the stereo projection correspond to the blue circles of Fig. 5, where the

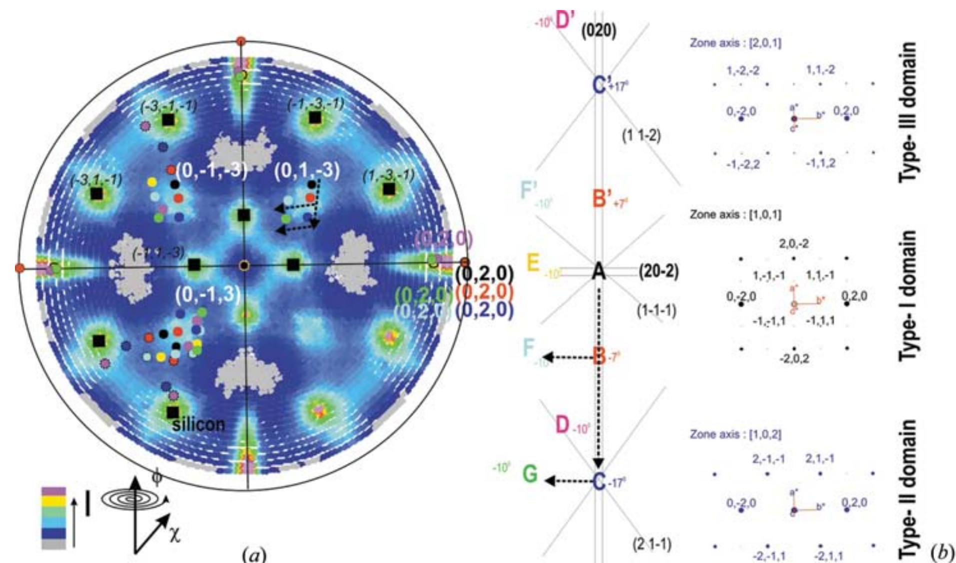

Figure 4
(*a*) (020)/(013) NiSi pole figure. Contributions from (131) planes of Si are also present (black squares). The lozenge-shaped patterns at $\chi = 45^\circ$ are due to (013) NiSi planes and the elongated patterns at the edges of the figure are due to the (020) planes of NiSi. (*b*) Schematic view of the domains forming the NiSi layer, with the corresponding diffraction patterns to identify the planes orientation. In the core of the type I domain ('A'), the (020) planes contribute to the pole figure at $\chi = 90^\circ$, $\varphi = 0^\circ$, while the diffracted spots from (013) planes lie within the lozenges of quadrants I and II (black circles). Moving from 'A' to another region of the domains, the diffracted spots distribute as shown by the corresponding coloured circles. Note that they accumulate in the region of the lozenges and at the edges of the figure according to the symmetry of the substrate.

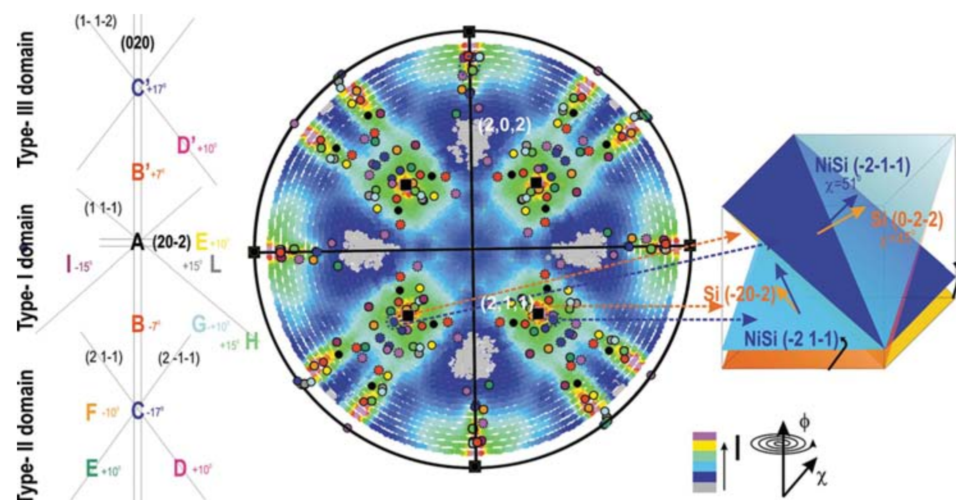

Figure 5
(*a*) (202)/(211) NiSi pole figure. Contributions of Si (220) planes are also present (black squares). Following the domain structure (left side schematic), some representative contributions from the NiSi lattice have been represented in the pole figure as coloured circles. Note that the (202) planes of NiSi tend to cover the features at the edge of the figure and the contribution from (211) planes accumulated within the lozenge in proximity to the Si signals and also along the splitting arms. Owing to the mutual position of these planes within the lattice of NiSi, the relationship with Si is such that when one of these NiSi planes approaches the core of the lozenge, the other in the near quadrant moves quite far away. This extreme configuration is not favorble. Instead, one of the most favorable locations of the NiSi planes with respect to the Si lattice is sketched on the right-hand side of the figure.

diffracted intensity is high. Therefore, this very peculiar configuration is real and extremely frequent.

4. Conclusions

It has been shown that NiSi tightly adapts to silicon by means of *transrotational* domains. Within the domains, the NiSi lattice establishes a double ordered relationship with silicon, in which (211) NiSi planes tend to match (220) Si planes in the proximity of $\chi = 45^\circ$ and $\varphi = 45, 135, 225$ and 315°. However, due to the disallowed match between the orthorhombic and the cubic lattice, the NiSi lattice has a certain degree of 'distortion' with respect to Si along χ and φ. The measure of these distortions is given by the bending of the domain and, therefore, by the extension of the related diffraction patterns in the pole figures. Each NiSi domain has, indeed, grown following the trace of the substrate and this phenomenon is related to the fact that Ni diffuses into Si to form NiSi.

In view of our findings, we believe that the driving force to grow these *transrotational* domains is the gain in volume rather than in the surface energy contribution. The Ni thickness becomes a critical parameter to tailor the growth process of the silicide since we do not observe *transrotational* domains for a 24 nm thick layer. In this respect, the kinetics of NiSi formation *versus* layer thickness is still under investigation, since the formation of transrotational domains have relevant implications on the scaling of NiSi layers which are currently used as metallizations for electronic devices.

This work has been partially supported by the European Project Impulse (IST-2001-32061).

References

Chen, L. J. & Tu, K. N. (1991). *Mater. Sci. Rep.* **6**, 53–140.
Choi, C.-J., Ok, Y.-W., Hullavarad, S. S., Seong, T.-Y., Lee, K.-M., Lee, J.-M. & Park, Y.-J. (2002). *J. Electrochem. Soc.* **149**, G517–G521.
Detavernier, C., Özcan, A. S., Jordan-Sweet, J., Stach, E. A., Tersoff, J., Ross, F. M. & Lavoie, C. (2003). *Nature (London)*, **426**, 641–645.
Detavernier, C. & Lavoie, C. (2004). *Appl. Phys. Lett.* **84**, 3549–3551.
Kolosov, V. Y. & Thölen, A. R. (2000). *Acta Mater.* **48**, 1829–1840.
Kooi, B. J. & De Hosson, J. Th. M. (2002). *J. Appl. Phys.* **92**, 3584–3590.
Kooi, B. J. & De Hosson, J. Th. M. (2004). *J. Appl. Phys.* **95**, 4714–4721.
Kooi, B. J., Groot, W. M. G. & De Hosson, J. Th. M. (2004). *J. Appl. Phys.* **95**, 924–932.
Lauwers, A., Steegen, A., Potter, M., Lindsay, R., Satta, A., Bender, H. & Maex, K. (2001). *J. Vac. Sci. Technol. B*, **19**, 2026–2037.
Lauwers, A., Kittl, J. A., Van Dal, M. J. H., Chamirian, O., Pawlak, M. A., de Potter, M., Lindsay, R., Raymakers, T., Pages, X., Mebarki, B., Mandrekar, T. & Maex, K. (2004). *Mater. Sci. Eng. B*, **114–115**, 29–41.
Lavoie, C., D'Heurle, F. M., Detavernier, C. & Cabral Jr, C. (2003). *Microelectron. Eng.* **70**, 144–157.
Lee, T. L., Lee, J. W., Lee, M. C., Lei, T. F. & Lee, C. L. (2003). *Electrochem. Solid-State Lett.* **6**, G66–G68.
Ok, Y.-W., Choi, C.-J. & Seong, T.-Y. (2003). *J. Electrochem. Soc.* **150**, G385–G388.
Teodorescu, V., Nistor, L., Bender, H., Steegen, A., Lauwers, A., Maex, K. & Van Landuyt, J. (2001). *J. Appl. Phys.* **90,** 167–174.
Wong, A. S. W. *et al.* (2002). *Appl. Phys. Lett.* **81,** 5138–5140.